Particle-hole symmetry breaking in the pseudogap state of $Pb_{0.55}Bi_{1.5}Sr_{1.6}La_{0.4}CuO_{6+\delta}$: A quantum chemical perspective

Itai Panas

Department of Chemistry and Biotechnology, Chalmers University of Technology, SE-412 96 Gothenburg, Sweden

(Received 19 May 2010; published 24 January 2011)

Two Bi2201 model systems are employed to demonstrate how, beside the Cu-O σ band, a second band of purely O $2p_\pi$ character can be made to cross the Fermi level due to its sensitivity to the local crystal field. This result is employed to explain the particle-hole symmetry breaking across the pseudogap recently reported by Shen and co-workers [see M. Hashimoto *et al.*, Nature Phys. **6**, 414 (2010).]. Support for a two-bands-on-a-checkerboard candidate mechanism for high-T_c superconductivity is claimed. Analysis based on band structures, partial density of states, and sum over states densities scanning-tunneling-microscopy-type images is provided.

DOI: 10.1103/PhysRevB.83.024508 PACS number(s): 74.72.−h, 71.18.+y, 71.20.Ps

I. INTRODUCTION

Generic electronic-structure features of hole-doped cuprate superconductors are presently being exposed at a renewed and even accelerating pace. The emerging consensus is that two energy gaps coexist in an electronically highly inhomogeneous state of matter. The gaps are associated with the superconducting state and a pseudogapped state,[1] respectively. The pseudogap function is discriminated by the fact that it displays only minor changes above and below the critical temperature for superconductivity. The ongoing progress is made possible by the combination of insights gained from the *real-space* scanning-tunneling-microscopy/scanning-tunneling-spectroscopy (STM/STS) technique[2–8] and *reciprocal-space* angle-resolved photoemission spectroscopy (ARPES).[9–20] These complementary techniques have acquired impressive precision over the years, partly driven by the unsolved riddle of high-T_c superconductivity (HTS) found in said cuprates. Their success is proposed later in the paper to reflect fundamental complementarities inherent in the underlying physics of the HTS phenomenon.

One contemporary phenomenological perspective on the HTS property has the pseudogap state and the superconducting state reflecting two competing phases; see, e.g., Refs. 9 and 10. A complementary possible understanding is that the pseudogapped state signifies a segregated "preformed" pairs phase.[11–13] A popular conceptual microscopic framework is the Anderson resonating valence bond (RVB) model[21–23] based on the Gutzwiller method[24] akin to the treatment by Rice and Ueda[25] of the periodic Anderson model[26] for heavy fermions. Here, a charge-carrier segregated reference system, as manifested in the checkerboard structure, could be understood to act as an in-plane charge buffer for the hole-doped antiferromagnetic (AFM) subsystem, allowing the superconductor (SC) to fine-tune the AFM doping via the Anderson hybridization term.

A complementary microscopic viewpoint is explored. It is a straightforward conceptual extension to said interpretation of the Anderson RVB model, but rather than solely providing hole buffering sinks, the hole-segregated plaquettes become entangled by interplaquette interactions reflecting the sharing of pair states, that is, Cooper pairs, as mediated by virtual magnons in the doped AFM embedding.[27–29] The rigidity of interplaquette entanglement is reflected in the SC gap function, while the rigidity of the virtual pair-susceptible AFM medium is reflected in the pseudogap function, which becomes renormalized due to the appearance of the former. This conceptual understanding is reminiscent of a spinon-holon terminology (see Refs. 21–23), where the spin-charge separation quality is replaced by the assumption that *neither* local spin *nor* local space symmetry are valid local descriptors in either the local AFM medium or the plaquette separately. It is the fact that the AFM + plaquette compound system *does* preserve local spin and symmetry *in conjunction with* the spatial extension of local AFM that enforces the entangled plaquettes' ground state.

In light of this, any new information regarding the properties of the pseudogap is met with the utmost interest. Recently, the temperature evolution of the pseudogap was mapped out in detail by means of ARPES in terms of signatures of the band structure at the Fermi level in the vicinity of the superconducting gap function antinodal direction.[20] That study succeeded in monitoring the opening of the pseudogap, and even more interestingly, it claimed to demonstrate fundamental particle-hole asymmetry (PHA). Phenomenological modeling based on the sufficiency of charge-carrier segregation in the form of periodic checkerboard superstructures to achieve the PHA was attempted in Ref. 20. What adds to the drama is that the opening of a gap in a single-band scenario, that is, single-band Peierls instability,[30] does not *per se* render PHA. At least a two-band physics is required. Because conventional theory implies particle-hole symmetry conservation across the SC gap, the observed PHA across the pseudogap is effective in discriminating between the pseudogapped state and the superconducting state. However, this argument is equally valid in excluding the previously mentioned Peierls-type charge-density wave (CDW) as a candidate for the pseudogapped state. What is required for the particle-hole asymmetry is the existence of nonequivalent particle sink and source states. Such a situation may indeed be inferred from one of the central dogmas in contemporary HTS theory, that is, the validity of the local-density approximation (LDA) band structure in providing a general basis for interpretation of the HTS phenomenology in terms of the in-plane Cu-O σ bands; see, e.g., Refs. 31–33. In these models, the required two bands for

particle-hole asymmetry would comprise the upper and lower Hubbard bands, the former acting as an electron sink and the latter as an electron source. Assumed instability toward hole segregation would result in the checkerboard observed directly by STM and indirectly as anomalous spectral broadenings in ARPES.

The purpose of the present study is to propose the complementary view to said upper-lower Hubbard band phenomenology. Hence, sufficient conditions for the hole-doped lower Hubbard band to act as an electron sink and a pure in-plane oxygen band of O $2p_\pi$ character to take the role of an electron source are demonstrated. Such a redistribution of holes can occur due to the innate inhomogeneous crystal fields as well as by the attenuation of the crystal field as caused by the displacement of cations relative to the CuO_2 planes. The two model compounds $Bi_{1.5}$,$Pb_{0.5}Sr_{1.5}$,$La_{0.5}CuO_6$ and $Bi_2Sr_2CuO_6$ are employed here to demonstrate the two cases, respectively. In what follows, the contextual implications of our complementary understanding will first be reiterated. Second, the influence on the resulting band structure of the relative positions of the dopants Pb^{2+} and La^{3+} replacing Bi^{3+} and Sr^{2+}, respectively, is demonstrated. Interpretation is provided by STM-type images generated by sum over states densities in the vicinity of the Fermi level. Third, the corresponding effects due to displacement of Sr^{2+} positions in pure $Bi_2Sr_2CuO_6$ will be demonstrated by band-structure calculations in conjunction with partial density of states (PDOS) analysis and STM-type images. Finally, the proposed two-band scenario on a checkerboard framework will be employed to interpret the central observations of Shen and co-workers.[20]

II. A MULTIBAND SCENARIO FOR HIGH-CRITICAL-TEMPERATURE SUPERCONDUCTIVITY

The scenario for HTS formulated earlier[27–29] includes three steps. (i) At elevated temperatures, mobile holes reside in the dispersive bands produced by the Cu-O σ states. (ii) Upon cooling, the charge carriers become trapped, such as with Zhang-Rice (ZR) singlets,[34] or are transferred into bands of O $2p_\pi$ character. Indeed, recovery of local antiferromagnetic coupling[35] requires such a transfer. The opening of the pseudogap has two contributions: one is the development of AF coupling among Cu $3d^9$ sites, and the second is the complementary clustering of holes in "superatom" states spanned by linear combinations of O $2p_\pi$ states. (iii) HTS emerges from a two-gapped "normal" state, such that resonant coupling of virtual hole cluster excitations and complementary virtual magnons contributes to the correlated ground state. Aspects of this understanding have been articulated in terms of a real-space analog[27] to the Bardeen-Cooper-Schrieffer theory, and in an equivalent two-component RVB Bose-Einstein condensation (BEC) formulation.[29] The latter implies that BEC among virtual hole cluster excitations is mediated by BEC of virtual magnons. Because the one provides the coupling required for the other to condense, the corresponding two signatures (superconductivity and spin-flip resonance[36]) appear at the same temperature, that is, at T_c. Our physical understanding[27–29] is similar to that of Ref. 37. Yet the realization of said physics is different both with regard to the detailed mechanism and in the fundamental two-band origin of the electronic structure subject to segregation of charge carriers. The understanding developed for the cuprates[29] was employed to formulate the superconductivity in FeSe,[30] that is, in terms of an analogous multiband scenario to that developed for the cuprates. While such complexity is generally accepted in the case of Fe-chalcogenides and Fe-pnictides, Cu-O σ-band (see, e.g., Ref. 38) scenarios still dominate in the case of cuprates. The report by Shen and co-workers[20] may provide the first solid ARPES-based evidence in favor of a multiband mechanism promoted by segregation in the case of HTS cuprates.

III. $Bi_{1.5}Pb_{0.5}Sr_{1.5}La_{0.5}CuO_6$ BAND-STRUCTURE DECONVOLUTION

Causes for the observations reported for $Bi_{1.5}Pb_{0.55}Sr_{1.6}La_{0.4}CuO_{6+\delta}$ in Ref. 20 are sought in the $Bi_{1.5}Pb_{0.5}Sr_{1.5}La_{0.5}CuO_6$ model system by means of spin-polarized general-gradient-approximation (GGA) Perdew-Burke-Enzenhofer (PBE) band-structure calculations. Taking the $Bi_2Sr_2CuO_6$ crystal structure as a point of departure, in what follows, the influences of different structural replacements of Sr^{2+}-Bi^{3+} pairs by La^{3+}-Pb^{2+} pairs on the resulting electronic structures are demonstrated.

In Fig. 1, we note that there are three distinctly different positions for the 25% replacement of Sr^{2+} by La^{3+}, and the 25% replacement of Bi^{3+} by Pb^{2+}. In all three cases, the density-functional-theory (DFT) ground state is a singlet. The band structures for the three cases are displayed in Figs. 2(a), 2(c), and 2(e). The most dramatic effect on the band structure due to the relative positions of Pb^{2+} and La^{3+} is seen in the vicinity of (π,π), where a band is shifted toward the Fermi level. To get a real-space representation of the electronic structure, sum over states densities is performed in the vicinity of the Fermi level at the two CuO_2 planes in the unit cell [see Figs. 2(b) and 2(d)]. It is evident that the surfacing band at (π,π) has significant O $2p_\pi$ character. Apparently, the destabilization increases with increased distance between one of the CuO_2 planes and the La^{3+} ion. Complementarily, the bands in the CuO_2 plane vicinal to the La^{3+} ion experience stabilization due to the strong local crystal field. It is noted how the particle-hole symmetry in the structure of Fig. 1(a) reflects the exclusivity of Cu-O σ bands crossing the Fermi level in the vicinity of $(0,\pi)$, as seen by inspection in Fig. 2(b). This property is retained for the CuO_2 plane experiencing the strong crystal field; see Fig. 2(d1). However, in the case of the CuO_2 plane experiencing the weak crystal field, clear particle-hole asymmetry emerges; see Fig. 2(d2). This is because the surfacing O $2p_\pi$ band in the vicinity of (π,π) renders the hole states O $2p_\pi$ character, while the particle states are still dominated by the bands crossings at $(0,\pi)$.

IV. EMPLOYING $Bi_2Sr_2CuO_6$ TO INTERPRET $Bi_{1.5}Pb_{0.5}Sr_{1.5}La_{0.5}CuO_6$

Also by comparing the band structure in Fig. 2 to that of native $Bi_2Sr_2CuO_6$ [Fig. 3(a)], it is clearly seen how bands in the vicinity of (π,π) along the $(0,\pi)$-(π,π) direction become

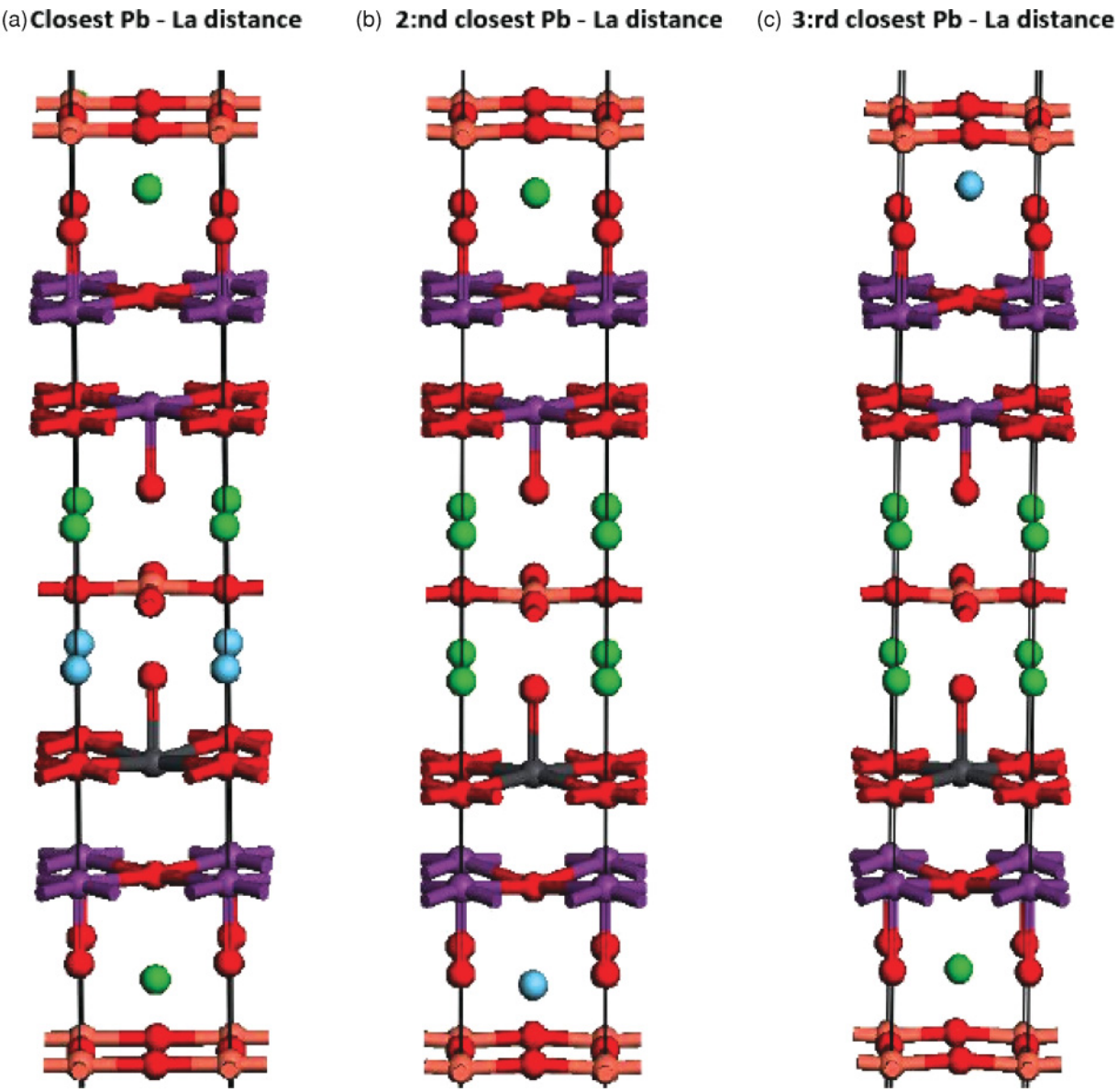

FIG. 1. (Color online) Crystal structures of $Bi_{1.5}Pb_{0.5}Sr_{1.5}La_{0.5}CuO_6$, where the position of the La^{3+} (light blue) with respect to the Pb^{2+} (gray) differs.

shifted toward the Fermi level in the case of the La^{3+}-Pb^{2+} doped samples. In addition, the apparent single Cu-O σ band that crosses the Fermi level halfway between (π,π) and (0,0) [see Fig. 3(a)] is seen to split upon partial replacement of Sr^{2+}-Bi^{3+} pairs by La^{3+}-Pb^{2+} pairs; compare Fig. 2(a) and Fig. 3(a). This reflects the inherently lower crystal-field symmetry of the former compound. The fact that this is a crystal-field effect is demonstrated by displacing two Sr^{2+} ions 0.1 and 0.2 Å away from one bracketed CuO_2 plane, thus artificially creating a weak-field–strong-field inhomogeneity between CuO_2 planes. The expected effect can be appreciated by comparing Fig. 3(a) to Figs. 3(c) and 3(e) at (π,π)-(0,0), where the Cu-O σ bands are seen to split.

Most importantly, it was reported that $Bi_{1.5}Pb_{0.5}Sr_{1.5}La_{0.5}CuO_6$ has characteristics of a band of O $2p_\pi$ character that may rise and touch the Fermi level in the $(0,\pi)$-(π,π) direction; see Fig. 2. It is gratifying to note and indeed it is emphasized how this phenomenon can be reproduced by artificial Sr^{2+} ion displacements in $Bi_2Sr_2CuO_6$; compare Figs. 3(a), 3(c), and 3(e) at (π,π). Indeed, in the case of Fig. 3(e), the attenuated local crystal field causes the formation of a hole pocket in the vicinity of (π,π). The fact that the surfacing band is of O $2p$ character is concluded from the PDOS plots; see Figs. 3(b), 3(d), and 3(f). Note, in particular, how the O $2p$ states pile up at the Fermi level in Fig. 3(f). The π character of the O $2p$ states is again extracted by taking the real-space complementary perspective offered by sum over states densities in the vicinity of the Fermi level, producing STM-type images at the CuO_2 planes experiencing the weak and strong local crystal fields; see Fig. 4. Clearly, the planes experiencing weak and strong crystal fields exhibit different characteristics. Similar to the case of $Bi_{1.5}Pb_{0.5}Sr_{1.5}La_{0.5}CuO_6$, the *strong local crystal fields* display bias-independent Cu-O σ-band character at the

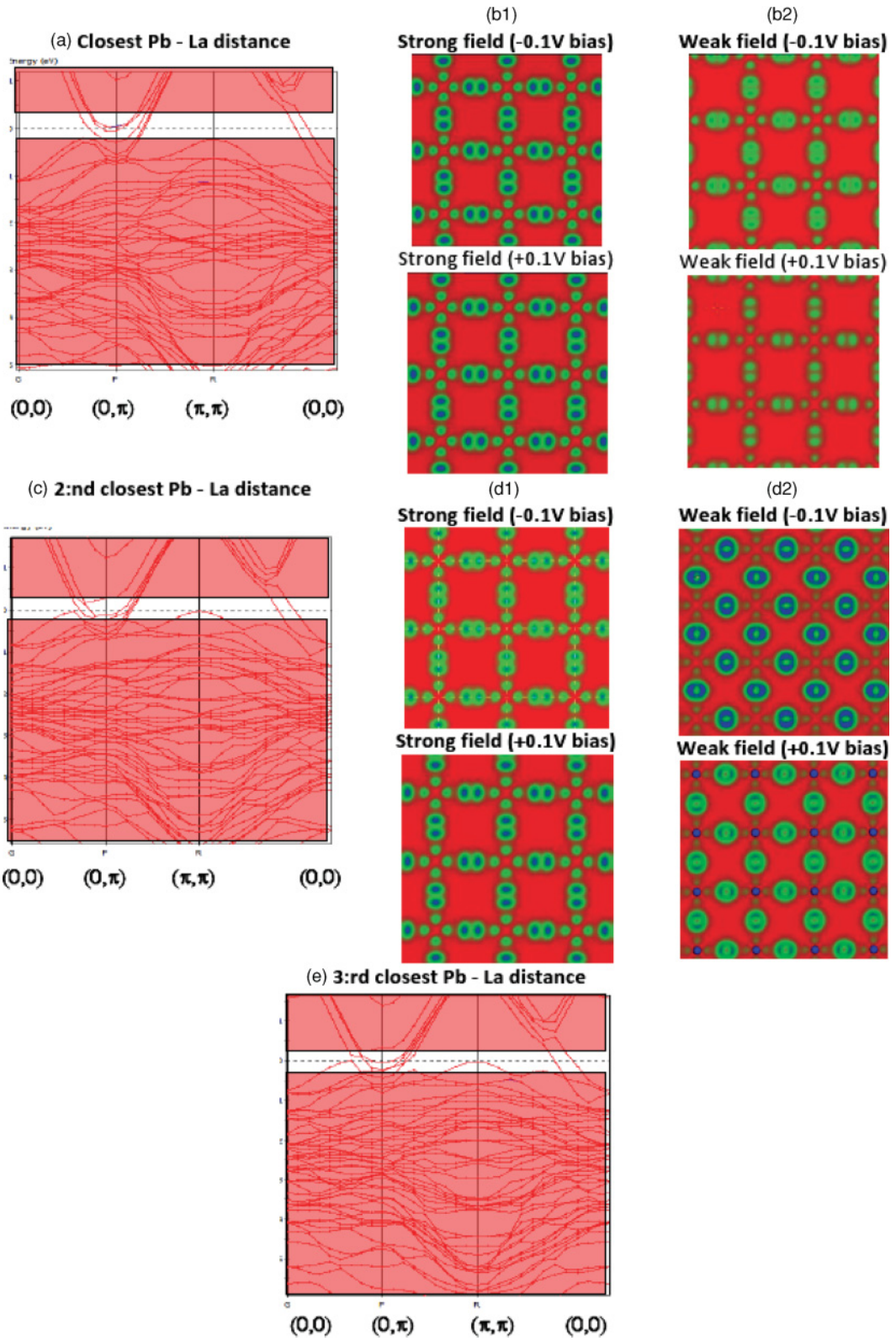

FIG. 2. (Color online) (a) In-plane band structure (0,0)-(0,π)-(π,π)-(0,0) corresponding to the structures in Fig. 1(a). (b) Sum over states densities STM-type images in the case of the CuO_2 plane, which experiences strong (b1) and weak (b2) local crystal fields, illustrating particle-hole symmetry in both cases. (c) In-plane (0,0)-(0,π)-(π,π)-(0,0) band structure corresponding to the crystal structures in Fig. 1(b). (d) Corresponding sum over states densities STM-type images in the case of the CuO_2 plane, which experiences strong (d1) and weak (d2) local crystal fields illustrating particle-hole symmetry in the former, while particle-hole asymmetry in the latter. (e) In-plane band structure (0,0)-(0,π)-(π,π)-(0,0) corresponding to the structures in Fig. 1(c).

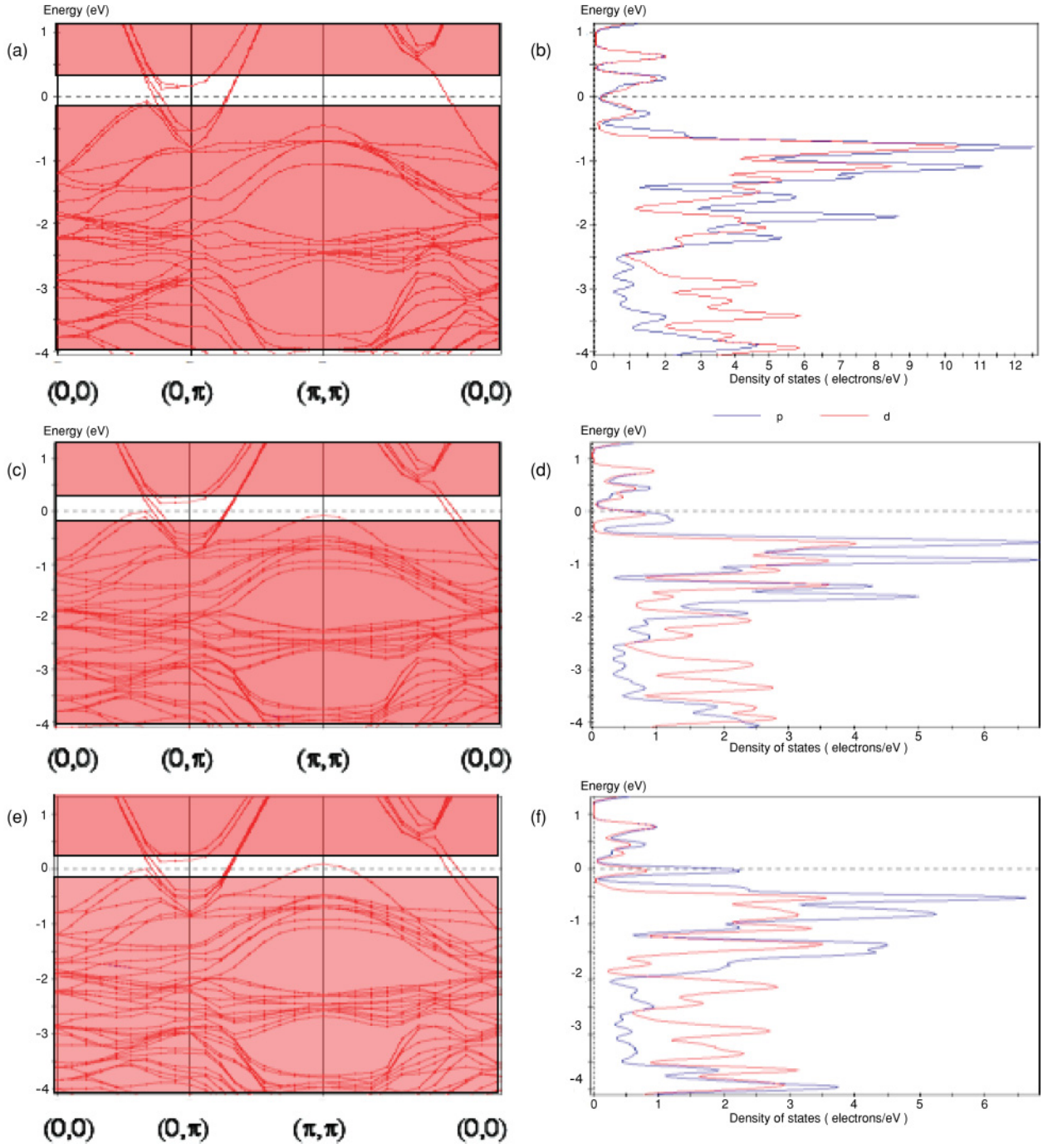

FIG. 3. (Color online) (a) Band structure and (b) CuO_2 PDOS for $Bi_2Sr_2CuO_6$ (compare Fig. 2). Also displayed are the band structure (c) and PDOS (d) for CuO_2 planes in $Bi_2Sr_2CuO_6$ caused to experience an artificially weak field (0.1 Å displaced Sr^{2+} ions; see text). (e) and (f) are the same as (c) and (d) but with 0.2-Å Sr^{2+} displacements. The PDOS display the Cu 3*d* (red) and O 2*p* (blue) contributions.

Fermi level, that is, qualitative particle-hole symmetry [cf. Figs. 4 (a1), (a2) and Figs. 4(c1), (c2)]. In the case of the CuO_2 plane experiencing *weak local crystal field*, the STM images acquire in addition significant O $2p_\pi$ character. For the 0.1-Å Sr^{2+} displacement, the particle-hole asymmetry observed qualitatively reproduces what was found for $Bi_{1.5}Pb_{0.5}Sr_{1.5}La_{0.5}CuO_6$ [see Fig. 2(d)]. In the case of 0.2-Å displacement, the hole pockets developing at (π,π) cause the particle-hole symmetry in the weak local crystal-field CuO_2 plane, and the characteristics of the O $2p_\pi$ states become further accentuated; cf. Figs. 4(d1) and (d2). Essential here is the change in character of the particle states from Cu-O σ in the case of strong crystal fields into O $2p_\pi$ in the case of weak local crystal fields. The possible consequences of hole-pocket instabilities are discussed later.

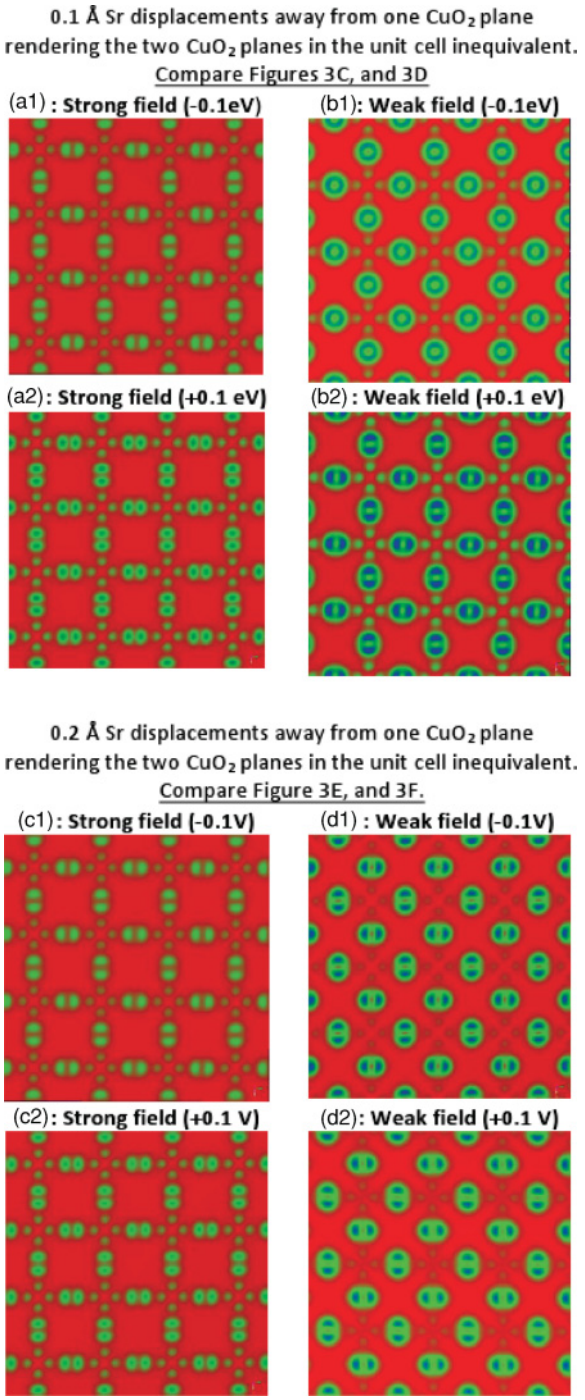

FIG. 4. (Color online) $Bi_2Sr_2CuO_6$ sum over states densities STM-type images corresponding to Fig. 3 (see text). STM-type images corresponding to the CuO_2 plane, which experiences the *unperturbed local crystal field,* comprise (a1) (−0.1-V bias; 0.1-Å displacement; CuO σ character), (a2) (+0.1-V bias; 0.1-Å displacement; Cu-O σ character), (c1) (−0.1-V bias; 0.2-Å displacement; Cu-O σ character), and (c2) (+0.1-V bias; 0.2-Å displacement; Cu-O σ character). STM-type images corresponding to the CuO_2 plane, which experiences the *weak local crystal field*, comprise (b1) (−0.1-V bias; 0.1-Å displacement; *mixed* Cu-O σ and O $2p_\pi$ character), (b2) (+0.1-V bias; 0.1-Å displacement; *mixed* Cu-O σ and O $2p_\pi$ character), (d1) (−0.1-V bias ; 0.2-Å displacement; O $2p_\pi$ character), and (d2) (+0.1-V bias; 0.2-Å displacement; O $2p_\pi$ character).

V. POSSIBLE CAUSE OF PARTICLE-HOLE ASYMMETRY ACROSS THE PSEUDOGAP

Having thus made a connection between the two employed model compounds, attention is given to the $(-\pi,\pi)$-$(0,\pi)$-(π,π) segment in the Brillouin zone, which was considered experimentally in Ref. 20.

The present interpretation assumes the Fermi surface of the hole-doped cuprates at $T > T^*$ to be well understood in terms of a hole-doped Hubbard-Mott insulator with a local Cu $3d^{9-\delta}$ electronic structure. Upon cooling, band shoulders at $\sim(\pm 0.1,\pi)$ appear at $T \sim T^*$ and become saturated at $\sim(\pm 0.2,\pi)$ for $T \ll T^*$. Here, this phenomenon is arrived at by first considering how upon cooling, crystal-field inhomogeneities cause the trapping of charge carriers. Indeed, the *a priori* symmetry-broken crystal field may be insignificant at elevated temperatures due to the high mobility of the charge carriers at those temperatures, but may become decisive below T^* and thus produce the observed temperature dependence of the ARPES signal. Secondly, this trapping acts to destabilize the holes *a priori* residing in the Cu-O σ bands. Thus, holes become partially transferred to the O $2p_\pi$ band. The destabilization of holes in Cu-O σ bands has two origins, of which one is the competing local AFM order and the second is the thermally modified crystal field destabilizing the O $2p_\pi$ band to the extent that it becomes a hole sink as manifested in the evolution of hole-pocket instabilities centered at (π,π). This understanding is summarized in Figs. 5(a) and 5(b), where the band folding is representative of twice doubling the unit cell to make a connection to the checkerboard superstructure. Figure 5(c) repeats the central part of Fig. 5(b) for the twice-folded O $2p_\pi$ band. A qualitative connection to the ARPES band structure at $T < T^*$ is made by tracing the occupied and unoccupied electronic states in Fig. 5(c). This is the cause of the claimed particle-hole asymmetry[20] understood to result from two disjoint bands crossing the Fermi level in conjunction with a four-unit-cell modulated stripe superstructure. The gap is due to two effects: (a) the stripes CDW in the O $2p_\pi$ band, and (b) the antiferromagnetic fluctuations. Assuming further stabilization of the Cu-O σ band and complementary destabilization of the O $2p_\pi$ band upon further cooling, it is indicated in Fig. 5(d) how the U-shaped Cu-O σ band is made to cross the first V-shaped segment of the O $2p_\pi$ band. This gives the resulting band an additional complexity, similar to that observed in Ref. 20, upon approaching the critical temperature for superconductivity.

It is emphasized that said stripes phenomenology is a spectator to the HTSC. Essential to the HTCS is how the hole-pocket instability at (π,π) of O $2p_\pi$ character has a bearing along the SC gap function nodal (0,0)-(π,π) direction. Indeed, a checkerboard superstructure, such as the generic charge-carrier segregated superlattice motif obtained for oxygen-doped Hg1201 (see, e.g., Fig. 6), is expected to produce additional Fermi-level crossing anomalies in the vicinity of both $(\pi/2,\pi/2)$ and $(\pi/4,\pi/4)$ due to the surfacing O $2p_\pi$ band. This provides a complementary conceptual framework for the interpretation of such observations,[19,39] contrasting, in particular, other proposed real-space inhomogeneities.[40] Indeed, the spectral broadening, taken in Ref. 20 to reflect electronic inhomogeneities, supports an interpretation along

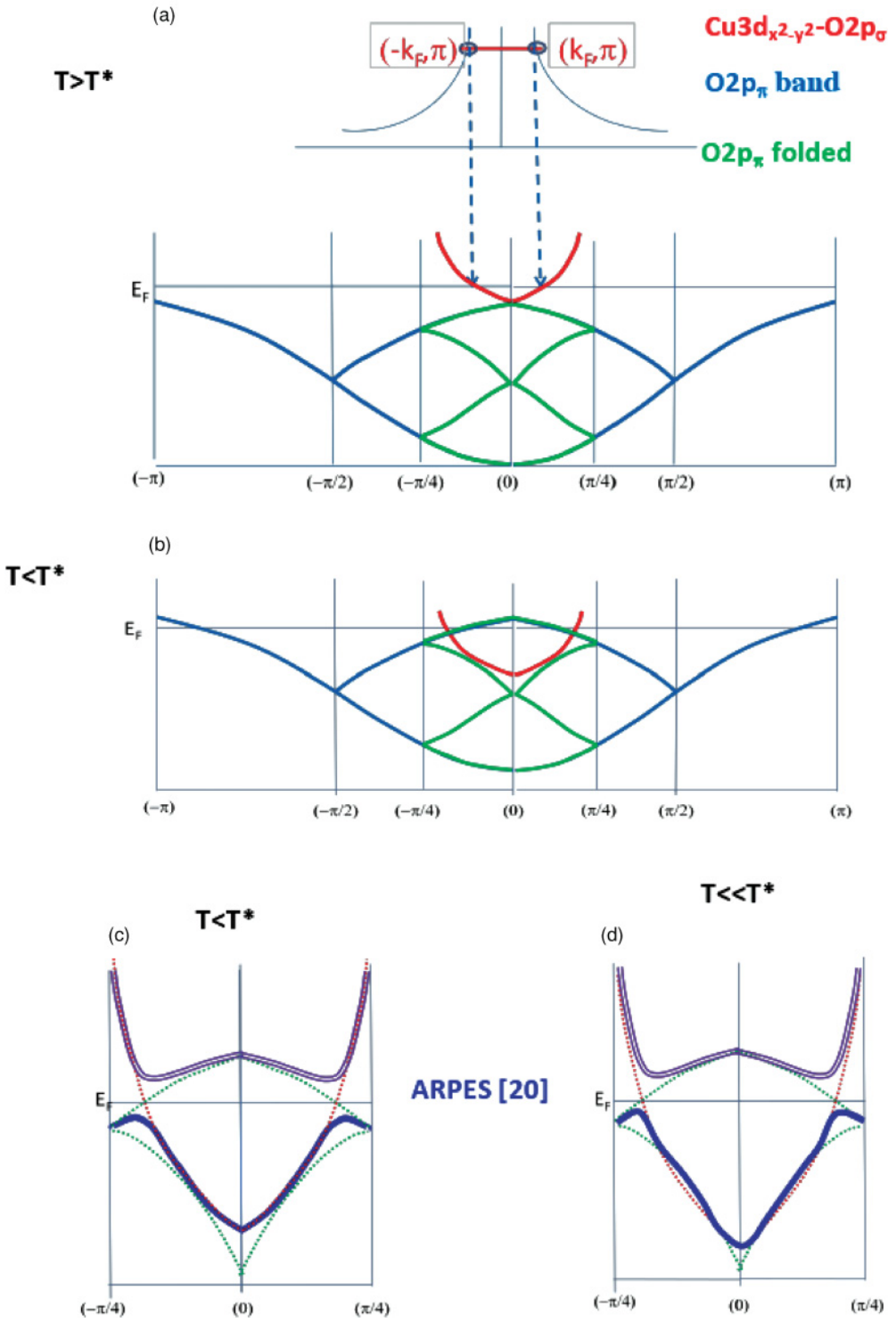

FIG. 5. (Color online) (a) Section probed by ARPES (Ref. 20) at $T > T^*$. The Cu-O σ conduction band (red) and the O $2p_\pi$ band (blue). The twice-folded O $2p_\pi$ band (green) assumes a four-unit-cell electronic modulation. (b) Stabilization of the Cu-O σ band (red) causes transfer of holes into the twice-folded destabilized O $2p_\pi$ band (green) ($T < T^*$). (c) Same as B. Cu-O σ band (dashed red). Twice folded O $2p_\pi$ band (dashed green). Effective hole states (blue) and particle states (purple) are indicated to make a connection to Ref. 20. (d) At $T < T^*$, the Cu-O σ band (dashed red) is suggested to cross the upper V-shaped segment of the twice-folded O $2p_\pi$ band (dashed green), giving the resulting band additional structural features (cf. Ref. 20).

the line suggested in Figs. 5 and 6. This is partly because (a) instability toward hole clustering is conditional for the low-dispersive O $2p_\pi$ bands to carry holes, and (b) ~25% random replacement of Sr^{2+} by La^{3+} and Bi^{3+} by Pb^{2+} is expected to cause random zero-dimensional charge-carrier attractors due to the inhomogeneous crystal field. It is emphasized

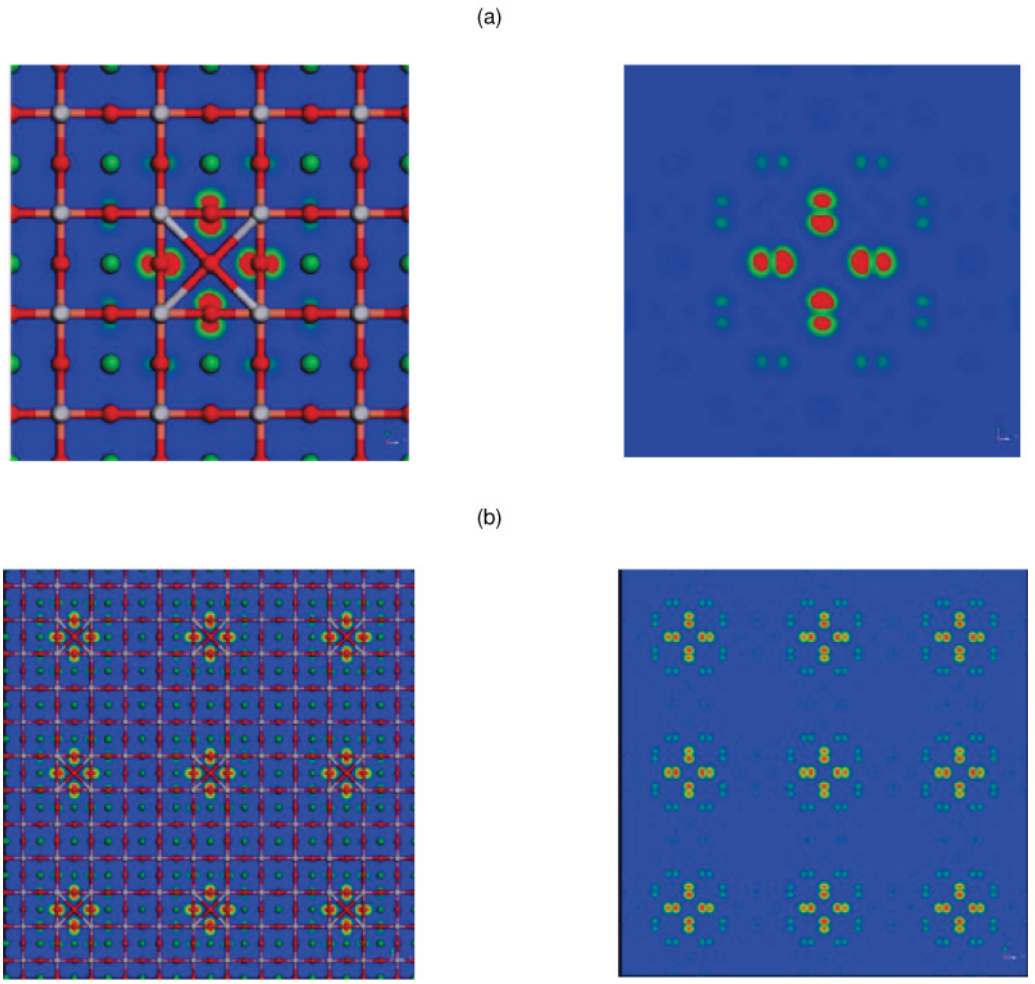

FIG. 6. (Color online) Hole clustering due to central δ-O in the Hg plane, producing a $4a_0 \times 4a_0$ supercell for Hg-1201. Sum-over-hole-states densities computed for -0.1-eV bias relative to the Fermi level. Note the O $2p_\pi$ character of the charge-carrier states in the vicinity of the Fermi energy. (b) Same as (a) but depicting 3×3 supercells to make a connection to a checkerboard structure.

that such charge-carrier segregations preserve the inherent near-degeneracy in the hole clusters due to the small O $2p_\pi$–O $2p_\pi$ orbital overlaps across the unit cell.[41] Note in Fig. 6 the apparent similarity to the ZR motif,[34] although in our case the Cu^{2+} ion, crucial to the ZR paradigm, is absent.

In conclusion, band structures, partial densities of states, and sum over states densities in the vicinity of the Fermi level have been employed to demonstrate sensitivity of the position of the O $2p_\pi$ band to local crystal field in two Bi2201 model systems to the extent that this band crosses the Fermi level in the vicinity of (π,π). This result was employed to propose an alternative interpretation of the particle-hole asymmetry across the pseudogap reported by Shen and co-workers.[20] The possible relevance of such an observation for HTS was discussed in the context of a quantum chemical formulation of high-T_c superconductivity,[27–29] the purpose of which is to serve as a conceptual tool for the discovery of new and improved superconducting materials.

VI. COMPUTATIONAL DETAILS

The band-structure calculations employ the CASTEP[42] program package within the Material Studios framework.[43] The GGA PBE functional[44] was employed. Core electrons were described by ultrasoft pseudopotentials,[45] O (6 electrons), Cu (11 electrons), Sr (10 electrons), La (11 electrons), Pb (14 electrons), and Bi (5 electrons), employing a 340-eV cutoff energy. Summations over the Brillouin zone employed a $7 \times 7 \times 1$ Monkhorst-Pack grid.[46]

ACKNOWLEDGMENTS

The author wishes to thank Tord Claeson and Øistein Fischer for stimulating discussions.

[1] T. Timusk and B. Statt, Rep. Prog. Phys. **62**, 61 (1999).
[2] Y. Kohsaka *et al.*, Science **315**, 1380 (2007).
[3] Y. Kohsaka *et al.*, Nature (London) **454**, 1072 (2008).
[4] J. E. Hoffman *et al.*, Science **295**, 466 (2002).

[5]M. Vershinin *et al.*, Science **303**, 1995 (2004).
[6]K. M. Shen *et al.*, Science **307**, 901 (2005).
[7]W. D. Wise *et al.*, Nature Phys. **4**, 696 (2008).
[8]W. D. Wise *et al.*, Nature Phys. **5**, 213 (2009).
[9]J.-H. Ma *et al.*, Phys. Rev. Lett. **101**, 207002 (2008).
[10]T. Kondo *et al.*, Nature (London) **457**, 296 (2009).
[11]T. Sato *et al.*, Phys. Rev. Lett. **103**, 047002 (2009).
[12]A. Kanigel, U. Chatterjee, M. Randeria, M. R. Norman, G. Koren, K. Kadowaki, and J. C. Campuzano, Phys. Rev. Lett. **101**, 137002 (2008).
[13]H.-B. Yang *et al.*, Nature (London) **456**, 77 (2008).
[14]M. Randeria *et al.*, Phys. Rev. Lett. **74**, 4951 (1995).
[15]J. Wei *et al.*, Phys. Rev. Lett. **101**, 097005 (2008).
[16]W. S. Lee *et al.*, Nature (London) **450**, 81 (2007).
[17]K. Tanaka *et al.*, Science **314**, 1910 (2006).
[18]R.-H. He *et al.*, Nature Phys. **5**, 119 (2009).
[19]J. Q. Meng *et al.*, Nature (London) **462**, 335 (2009).
[20]M. Hashimoto *et al.*, Nature Phys. **6**, 414 (2010).
[21]P. W. Anderson, Science **235**, 1196 (1987).
[22]G. Baskaran, Z. Zou, and P. W. Anderson, Solid State Commun. **63**, 973 (1987).
[23]G. Baskaran and P. W. Anderson, Phys. Rev.B **37**, 580 (1988).
[24]M. C. Gutzwiller, Phys. Rev. **137**, A1726 (1965).
[25]T. M. Rice and K. Ueda, Phys. Rev. Lett. **55**, 995 (1985).
[26]P. W. Anderson, Phys. Rev. 124 (1961).
[27]I. Panas, J. Phys. Chem. B **103**, 10767 (1999).
[28]I. Panas, Phys. Rev. B **82**, 064508 (2010).
[29]I. Panas (submitted to New J. Phys.).
[30]R. Peierls, *More Surprises in Theoretical Physics* (Princeton University Press, Princeton, NJ, 1991).
[31]H. Krakauer and W. E. Pickett, Phys. Rev. Lett. **60**, 1665 (1988).
[32]W. E. Pickett, Rev. Mod. Phys. **61**, 433 (1989).
[33]O. K. Andersen *et al.*, J. Phys. Chem. Solids **56**, 1573 (1995).
[34]F. C. Zhang and T. M. Rice, Phys. Rev. B **37**, 3759 (1988)
[35]R. Ofer, G. Bazalitsky, A. Kanigel, A. Keren, A. Auerbach, J. S. Lord, and A. Amato, Phys. Rev. B **74**, 220508(R) (2006).
[36]H. F. Fong, B. Keimer, D. L. Milius, and I. A. Aksay, Phys. Rev. Lett. **78**, 713 (1997).
[37]E. Altman and A. Auerbach, Phys. Rev. B **65**, 104508 (2002).
[38]E. Pavarini, I. Dasgupta, T. Saha-Dasgupta, O. Jepsen, and O. K. Andersen, Phys. Rev. Lett. **87**, 047003 (2001).
[39]S. E. Sebastian *et al.*, Phys. Rev. B **81**, 214524 (2010).
[40]Y. He, T. S. Nunner, P. J. Hirschfeld, and H. P. Cheng, Phys. Rev. Lett. **96**, 197002 (2006)
[41]I. Panas and R. Gatt, Chem. Phys. Lett. **259**, 241 (1996)
[42]S. J. Clark *et al.*, Z. Kristallogr. **220**, 567 (2005).
[43]Materials Studio 5.0, Accelrys Inc., simulation software.
[44]J. P. Perdew, K. Burke, and M. Ernzerhof, Phys. Rev. Lett. **77**, 3865 (1996).
[45]D. Vanderbilt, Phys. Rev. B **41**, 7892 (1990).
[46]H. J. Monkhorst and J. D. Pack, Phys. Rev. B **13**, 5188 (1976).